Digest Journal of Nanomaterials and Biostructures

Dig. J. Nanomater. Bios. **2026**; 21(2): 55320
https://doi.org/10.31083/DJNB55320

Original Research

Effect of Annealing on the Optical Properties of Copper Zinc Tin Sulfide (CZTS) Thin Films Deposited Using a Modified Successive Ionic Layer Adsorption and Reaction (SILAR) Method

Tahar Tahouri[1,2], Hamid Khachab[2], Faouzi Saidi[3], Abdelghani Laouer[4], Bernabé Mari Soucase[5], Mohamed Teggar[6], Naceur Selmane[1,7,*]

[1]Faculty of Technology Sciences, University Amar Telidji, 03000 Laghouat, Algeria
[2]Laboratory of Development Renewables Energys and Their Applications in Sahara Areas (LDREAS), Faculty of Exact Sciences, Tahri Mohammed University, 08000 Bechar, Algeria
[3]Laboratoire de Mico-Optoelectronique et Nanostructures, Faculté des Sciences, Université de Monastir, 5000 Monastir, Tunisia
[4]Departement of physics, Faculty of Exact Sciences and Computer Science, University of Jijel, 18000 Jijel, Algeria
[5]Instituto de diseño y Fabricación (IDF), Universitat Politècnica de València, 46022 València, Spain
[6]Laboratory of Mechanics, Laghouat University, 03000 Laghouat, Algeria
[7]Laboratoire Matériaux, Systèmes Énergétiques, Énergies Renouvelables et Gestion de l'Énergie (LMSEERGE), University Amar Telidji, 03000 Laghouat, Algeria
*Correspondence: n.selmane@lagh-univ.dz (Naceur Selmane)
Academic Editor: Haider Abbas
Submitted: 2 January 2026 Revised: 19 March 2026 Accepted: 26 March 2026 Published: 26 June 2026

Abstract

Copper zinc tin sulfide (CZTS) films deposited using a modified successive ionic layer adsorption and reaction (SILAR) method were annealed in air. Surface growth was examined using X-ray photoelectron spectroscopy and scanning electron microscopy. With a suitable orientation in plane (112) at 2θ = 27.88°, the films crystallized in a kesterite structure. The impacts of annealing temperature and time on film optical properties were investigated using absorption and transmission spectroscopy. Whereas SILAR-grown CZTS films usually exhibit a somewhat disorganized nanocrystalline structure and band gaps of 1.3–1.8 eV, annealing lowered the band gap to 1.4–1.5 eV and improved absorption while weakly affecting composition. The films annealed at 250 °C for 120 min had a band gap of 1.3 eV and at 250 °C for 90 min displayed advantageous optical properties, namely an optical band gap of 1.5 eV, refractive index of 2.9, high-frequency dielectric constant of 8.5, and static dielectric constant of 13.900. These results demonstrate the effectiveness of the modified SILAR deposition method.

Keywords: CZTS thin film; optical properties; SILAR deposition method; annealing parameters

1. Introduction

Due to rising energy demand, photovoltaic solar power output has increased dramatically in recent decades. Research has focused on developing low-cost, highly efficient photovoltaic panel manufacturing techniques [1]. Over the last two decades, kesterite-based Cu_2ZnSnS_4 (CZTS) materials have been intensively researched as substitutes for Cu (In, Ga) Se_2 (CIGS) and CdTe compounds in thin-film solar cells**.** Because of its remarkable characteristics, including earth-abundant and non-toxic materials, an ideal optical band gap (1.0–1.5 eV) [2], excellent absorption coefficients (>10^4 cm^{-1}) [3,4], attractive electrical properties, and appropriate optical band gap (1.0–1.5 eV), the CZTS has emerged as a viable absorber for thin-film-based photovoltaic applications [3]. More layers of thin-film absorbers, including CdTe and CIGS, for instance, have already attained conversion efficiencies of greater than 22% [1,5]. As per the Shockley-Queisser theory, theoretical simulations indicated that the p-n junctions based on CZTS have efficiencies more than 30% [6]. Currently, the "champion" efficiency for a physical device is 13.2% for pure sulfide CZTS and 14.9% for CZTSSe (the selenium-alloyed variant) [7]. Many factors may explain the disparity between theoretical and actual values, including secondary phase development during the growth process [8,9,10], inappropriate chemical composition [11,12], and the crystalline quality of the absorber layer [13,14]. As a result, optimizing annealing and deposition settings has a direct and considerable influence on CZTS-based solar cell conversion efficiency. Further study and development into CZTS solar cells and manufacturing methods is thus required to enhance their efficiency, because this will lead to CZTS photovoltaic cells which are playing a major role in advanced energy generation. In general, the thickness of the layer has an impact on the overall design of the gadget [15]. An ecologically acceptable and safe technique such as successive ionic layer adsorption and reaction (SILAR) deposition for creating kesterite thin films and controlling their thickness is important. This offers another method for making thin films for solar-cell use [16]. Our proposed

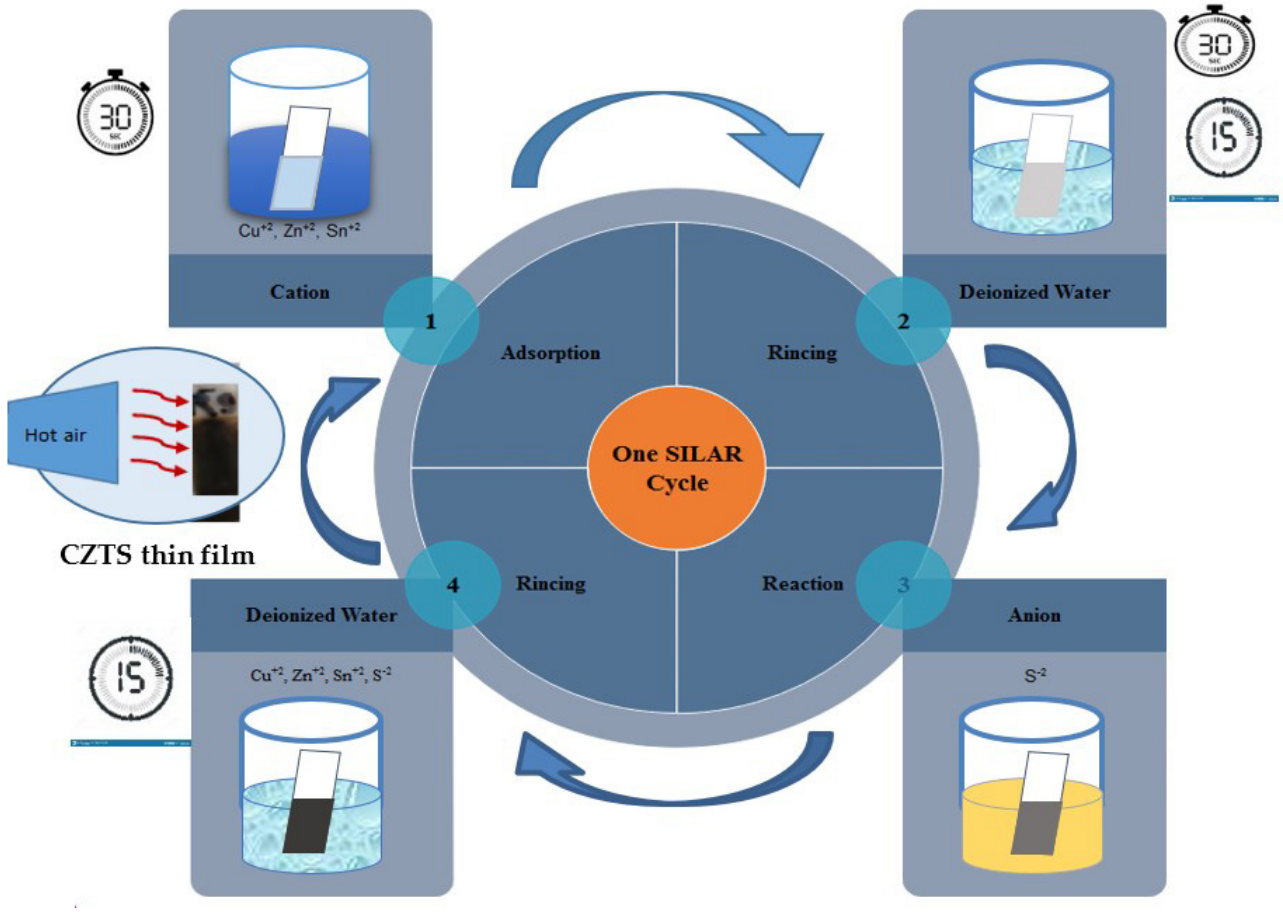

Fig. 1. The detailed schematic of modified SILAR. SILAR, successive ionic layer adsorption and reaction.

modification to the SILAR method is a direct response approach that, in our opinion, may address the main issues with previous non-vacuum procedures.

This new approach also provides other advantages, including affordability and ease of use. Thin films can be deposited onto large areas and can be reproducibly deposited in short times onto any type of substrate. The method enables energy savings by using low deposition temperature with no need for high vacuum. The film thickness and particle size and shape can be easily adjusted by modifying the cycle of deposition and controlling the annealing conditions. The stoichiometry of the deposited material can also be controlled by adjusting the precursor solution's concentration [17,18]. The current work indicates the efficiency of modifying the SILAR deposition method, where a new step (Figs. 1,2) is added to produce the appropriate thickness of CZTS film, with just a few cycles for use in photovoltaic cells.

The SILAR method has been used to synthesize several compounds, including CdS [19,20], Cu-Zn-S [21], Cu–Sn–S [22], ZnO [23,24], and $CuInS_2$ (CIS) [25]. Recently, kesterite-based photovoltaic devices and thin films for kesterite absorbers have been made using these compounds. In 1985, Ristov and his group were the first to report that thin films could be synthesized by the SILAR method [26], but Nicolau named it the same year [23]. ZnS and CdS thin films are deposited using this technique at room temperature on various substrates. In addition, it has recently been used in the synthesis of the fundamental thin film structure in solar cells through the immersion reaction cycle. There are two methods for preparing CZTS films with SILAR: the conventional one-step technique [27,28], and sequential stacking of sulphide layers [24].

In the SILAR approach, the researchers often focus on the temperature of the substrate or precursor solution baths, where the deposition temperature is the key driver of reaction kinetics and film shape. The bath or substrate temperature controls how the ions interact with the substrate in real time, where at low temperatures, the kinetic energy of the ions is low, in contrast with the annealing temperature, which occurs after deposition [29]. This phenomenon frequently results in a slow deposition rate and inadequate coverage because the ions lack the energy to identify stable "sites" on the substrate. Furthermore, lower temperatures generate "nanocrystalline" or practically amorphous predecessors. Although these appear smooth, they frequently shatter during the final sulfurization/annealing stage due to their low density.

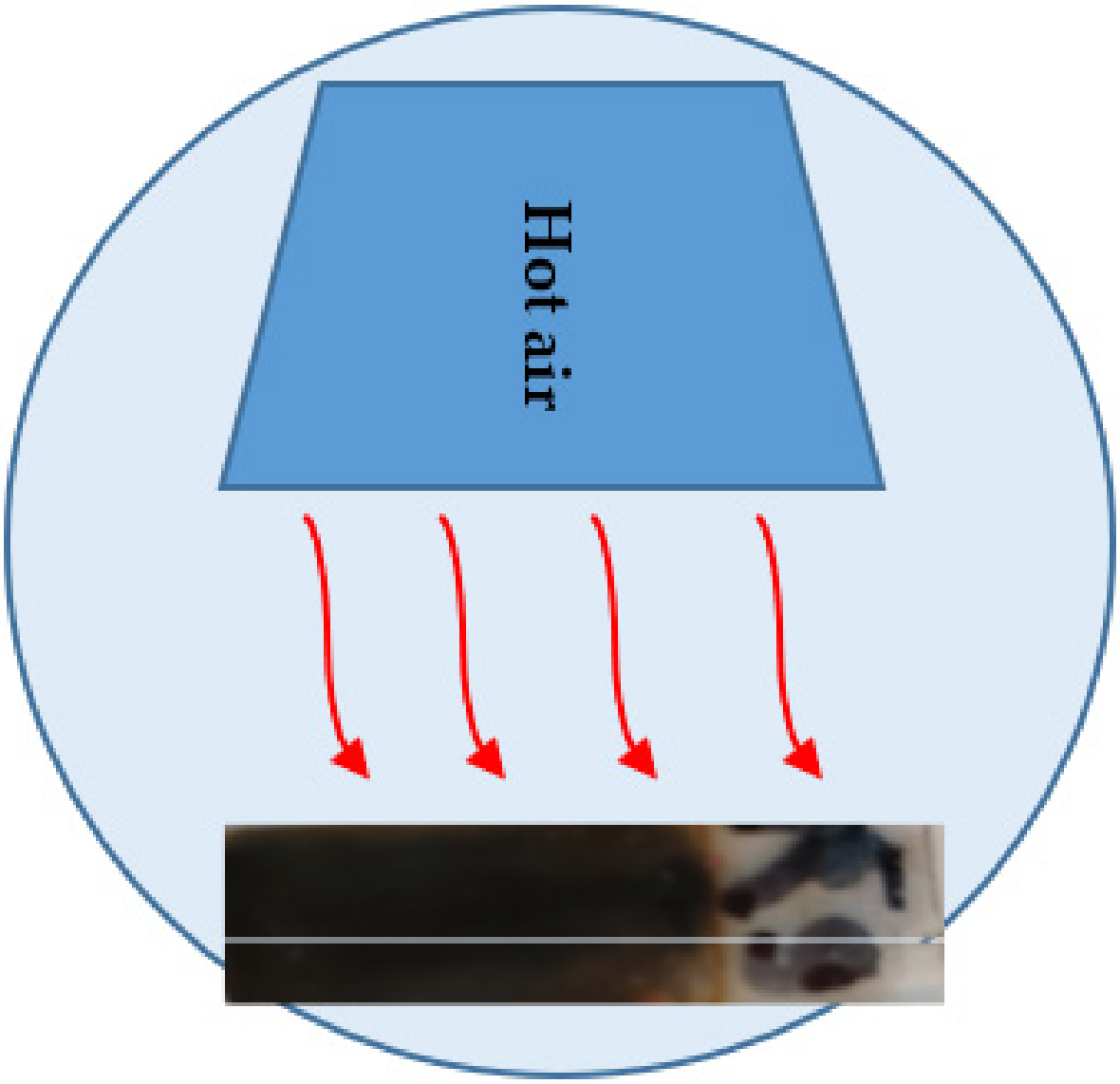

Fig. 2. The new step added to the SILAR method.

However, the "desorption" rate rises with increased bath temperature. The ions may bounce off the surface or detach before reacting with the next layer, resulting in extremely thin or discontinuous coatings. Additionally, higher bath temperatures encourage the development of larger initial nuclei. A film with bigger grain sizes and fewer grain boundaries is the outcome of this.

The "precipitation" issue may be the most important factor. In SILAR, a heterogeneous reaction—one that occurs on the substrate—is preferred over a homogeneous reaction—one that occurs in the beaker [30].

As a workaround and to get around the issue of the precursors' changing solubility as the temperature rises, in particular, the S ions (left over from earlier dives) immediately react with the Cu, Zn, and Sn ions in the liquid. Also, to address the issues of sluggish sedimentation rates and inadequate coverage at low temperatures, we chose to include the impact of temperature outside of the conventional framework of solution and substrate temperatures.

Most researchers focused on improving the properties of thin films using annealing after deposition because increasing the annealing temperature increases the mean grain size while decreasing the grain boundary density. Thus, there is less chance of electron scattering at grain boundaries, making it easier for electrons to go from the valence to the conduction band, which ultimately leads to a decreased band gap [25,31].

The present research shows how effectively annealing and deposition parameters (the time and the temperature) can be adjusted to produce the CZTS films with required thickness for usage in solar cells. To this aim, we have included the effect of temperature during deposition by the modified SILAR method in order to improve its effectiveness, where it was added in a one-step process at the end of

Table 1. A summary of all the information about the materials used in this work.

	CAS number	The manufacturer	
$CuCl_2$	7447-39-4	Sigma Aldrich	Saint Louis, MO, USA
$ZnSO_4$	7733-02-0	Sigma Aldrich	Merck KGaA, Darmstadt, Germany
$SnCl_2$	7772-99-8	Sigma Aldrich	Saint Louis, MO, USA
Na_2S	1313-82-2	Sigma Aldrich	Saint Louis, MO, USA

each cycle (see Fig. 2). Hot air is passed over the substrate to increase the cohesion and homogeneity of the thin layers before washing them again. This would resolve some significant difficulties that most researchers seek to overcome, resulting from the high or low temperature of the deposition process, which we mentioned above. Therefore, we have obtained thick layers in a few cycles with good crystallinity at a lower cost. To get rid of the problem of the complicated reaction route while annealing in the atmosphere of S or Se at a high temperature, we insisted that we perform the annealing process in the air at a medium temperature of 150 to 300 ºC in all our experiments.

2. Materials and Methods

Chemically pure copper (II) chloride ($CuCl_2 \cdot 2H_2O$, >99%), zinc sulfate ($ZnSO_4 \cdot 7H_2O$, >99.5%), tin (II) chloride ($SnCl_2 \cdot 2H_2O$, >97.5%) and sodium sulfide (Na_2S). Table 1 summarizes all of these materials' information.

Every reagent was used exactly as it was given. Deionized (DI) water was utilized to make aqueous solutions. Highly transparent indium tin oxide (ITO/glass surface), (In_2O_3 and (SnO_2) ratio 90:10 with surface resistivity 8–12 Ω/sq, CAS Number: 50926-11-9, Sigma Aldrich, Saint Louis, MO, USA) films were used as substrates to deposit the CZTS films.

Experimental Setup

Before the CZTS thin film being deposited, the ITO-coated glass substrates were cut into 1 × 2.5 cm^2, ITO Substrates were ultrasonically cleaned for 10 minutes using ethanol, acetone, and de-ionized water. The identical cycle was repeated several times. Finally, the substrate was dried before deposition. In the typical deposition, to avoid pre-capitation, substrates were soaked individually in solutions of anion and cation precursors, with simultaneous washing with DI water after each immersion. Initially, cationic ions (Cu^{+2}, Zn^{+2}, and Sn^{+4}) were adsorbed on the ITO substrate by vertically submerging the cleansed substrate in the solution of the cationic precursor for 30 seconds. Consequently, to get rid of the loosely attached ions, the substrate was rinsed with DI water for 10 seconds. It was then submerged in the anionic precursor solution for 30 seconds, during which time the anions (S^{-2}) reacted with the pre-adsorbed cations to create the CZTS layer on an ITO substrate. Lastly, the substrate was rinsed using DI water for 10 seconds in order to take off the loosely bonded, powdery CZTS particles and cation ions that hadn't reacted. In most studies, variations have been made to the preparative parameters, such as the number of cycles, dipping duration, and precursor concentration. In order to produce high-quality CZTS thin films, the films that were deposited were annealed at various suitable temperatures. During this work, the following was the typical recipe (2:1:1:4). The first beaker contained 0.02 M $CuCl_2$, 0.01 M $ZnSO_4$, and 0.02 M $SnSO_4$ solutions dissolved in 40 mL of DI water, to give (Cu^{+2}, Zn^{+2}, and Sn^{+4}) cations. When the substrate was immersed in the 1st beaker, these cations were adsorbed. In beaker 3, 0.16 M Na_2S was dissolved in the same volume of DI water, to give (S^{-2}) anions, where the thin film deposition process has ion-by-ion growth kinetics, which involved ion deposition at nucleation sites on immersed surfaces. According to Shinde et al. [32], nucleation occurred by adsorption of colloidal ions, and growth occurred through surface coagulation of these ions, resulting in a thin and adherent layer.

By repeatedly immersing the substrates in anionic and cationic precursor solutions and rinsing them in deionized water after each immersion, for 10 seconds, hot air was then passed over the substrate to increase the cohesion and homogeneity of the thin layers before immersing them again. With this new step, we obtained thick layers in a few cycles with good crystallinity at a lower cost. The modified SILAR method yielded uniform and well-adherent CZTS layers on ITO substrates. The primary chemical reaction that occurred during this cycle can be summarized by Eqns. 1,2,3,4.

$$CuCl_2 \rightarrow Cu^{+2} + 2Cl^{-1} \tag{1}$$

$$ZnSO_4 \rightarrow Zn^{+2} + SO_4^{-2} \tag{2}$$

$$SnCl_2 \rightarrow Sn^{+2} + 2Cl^{-1} \tag{3}$$

$$Na_2S \rightarrow 2Na^{+} + S^{-2} \tag{4}$$

The final ionic reaction is shown in Eqn. 5:

Table 2. XRD inspections of SILAR-deposited CZTS thin film deposited in 50 cycles.

CZTS of 50 cycles	2 Theta	d	FWHM full width at half maximum	Crystal size	kesterite phase	δ Dislocation density	ε micro-strain	Lattices parameters		
	deg	(Å)	deg	(nm)		(nm-2.10-3)		a (Å)	c (Å)	v (Å^3)
	27.88	3.19	0.30	29.06	(112)	1.184	0.059			
	32.09	2.78	0.73	11.91	(200)	7.049	2.083	5.54	10.93	335.46
	46.30	1.95	0.50	18.08	(220)	3.059	0.218			

$$2Cu^{+2} + Zn^{+2} + Sn^{+2} + 4S^{-2} \rightarrow Cu_2ZnSnS_4 \quad (5)$$

The substrate was successively immersed in the appropriate precursors for a few cycles, resulting in the thin layers of CZTS films shown in the examined samples. The resulting CZTS film transmittance and absorption varied depending on time and annealing temperature.

3. Results

3.1 Structure Properties

To evaluate the structural characteristics of CZTS nanoparticles, X-ray diffraction measurements were collected at 2θ values varying from 15º to 60º diffraction angles and using λ = 1.54056 Å. Fig. 3 illustrates the X-ray diffractometer (XRD) diagram of the tetragonal-structured CZTS films deposited with immersion cycles of 30, 40, and 50 cycles, respectively named as CZTS-30, CZTS-40, and CZTS-50. Using the modified SILAR method (Figs. 1,2), four prominent diffraction signals can be seen in the XRD pattern at 2θ values of 27.88º, 32.09º, 46.30º, and 54.97º attributed to reflections about (112), (200), (220), and (312) planes of the CZTS kesterite structure, respectively. Which corresponds to the kesterite CZTS structure (ICDD-ref.: 00-034-1246). In addition, there are other signals at 2θ = 21.40º, 30.42º, 35.31º, and 50.71º assigned to reflections from (211), (222), (400), and (440) planes, respectively, in annealed samples. These reflections in all samples correspond to the ITO layer (cubic structure In_2O_3) nanocrystals, and the pure phase patterns may be accurately referenced to all of the signals (JCPDS card No. 6-0416) [33,34].

In general, XRD signal positions give important structural information about CZTS films. However, to get accurate information about secondary phases, you need to carefully interpret them and use other methods [35].

The CZTS-50 samples were obtained after 50 cycles; their structural, compositional, and morphological characteristics were examined. With the findings listed in Table 2, emphasis was placed on them because they were most obvious. The production of CZTS with a kesterite structure and the lattice constants *a* = 5.54A and *c* = 10.93A were verified using XRD. At the apex, the average size of the crystallite was 29.06 nm (1 1 2).

Using the relationships Eqn. 6 and Eqn. 7 [36], for the films having a tetragonal structure, the determined lattice constants *a* and *c* were obtained [37].

$$a = \frac{\lambda}{2sin\theta}\sqrt{h^2 + k^2 + l^2\left(\frac{a}{c}\right)^2} \quad (6)$$

$$c = \frac{l}{\sqrt{\frac{h^2+k^2}{a^2} + \left(\frac{2sin\theta}{\lambda}\right)^2}} \quad (7)$$

The size of the crystallite was determined using Scherrer's formula [38], Eqn. 8:

$$D = \frac{K\lambda}{\beta cos\theta} \quad (8)$$

where K = 0.94: is the crystal form factor, λ = 1.54056Å: is the wavelength of X-ray, β: is full width at half maximum (FWHM), and θ: is the diffraction angle.

On the other hand, stresses [39], are among the most significant adverse effects on the structural characteristics that could arise from a geometric mismatch at the borders between the substrate and the crystalline lattices of films, and can consequently cause microstrain (e) in the films at that location. The microstrain ε may be found using Eqn. 9 [36]:

$$\epsilon = \frac{FWHM}{tng\theta} \quad (9)$$

Dislocation is one of the most significant flaws in a crystal, and the misregistry of the lattice in one area of the crystal is connected to that. Williamson and Smallman's relationship, Eqn. 10, was used to compute the thin-film dislocation density [40],

$$\delta = \frac{1}{D2}\left(lin\ e\ s\ /m^2\right) \quad (10)$$

where D is the crystalline size.

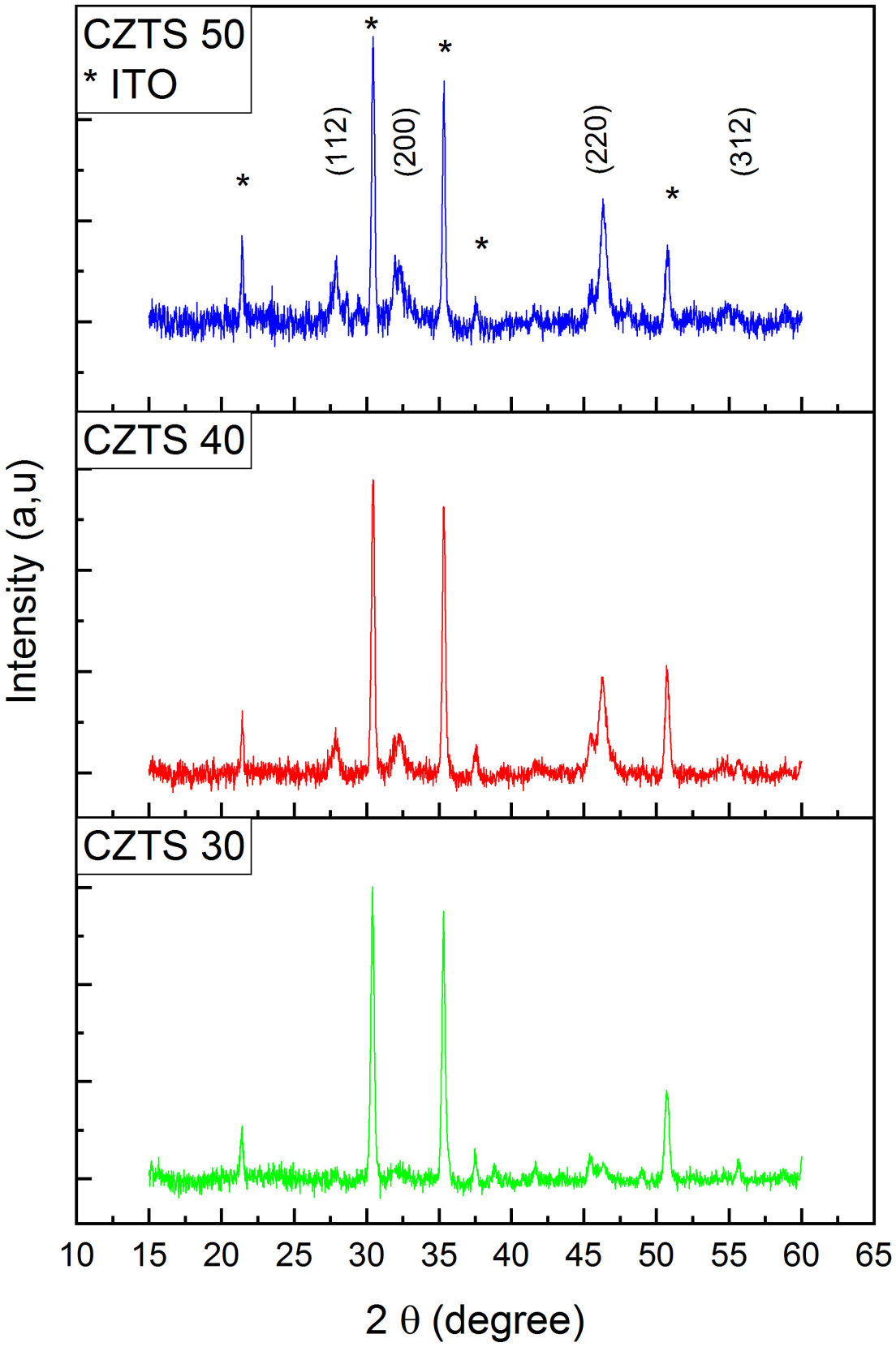

Fig. 3. XRD patterns of CZTS nanoparticles of different cycles annealed at 250 °C. CZTS, Cu_2ZnSnS_4, ITO, indium tin oxide; XRD, X-ray diffractometer.

The formula, Eqn. 11, can be used to determine the cell volume,

$$v = a^2 c \tag{11}$$

The dislocation was lower for the samples deposited with a higher number of cycles, as CZTS-50. It suggests that there are fewer lattice defects and less strain in these samples [41]. The formula was used to determine the dislocation density Eqn. 10 [42].

Table 2 summarizes the crystallite number, size, micro-strain, and dislocation density for the (2 2 0) orientation. The kesterite structure of CZTS films exhibited lattice values of a = 0.554 nm and c = 1.093 nm.

3.2 Surface Morphology

The surface morphology of all CZTS thin films at different annealing parameters underwent scanning electron microscopy (SEM) qualitative analysis. Fig. 4 shows the surface micrographs of CZTS thin films that have been annealed at various temperatures. The films exhibited generally homogeneous, densely packed surfaces on the ITO substrate that are free of cracks and well-coated. The development of agglomerations with well-defined borders was caused by increasing temperatures and annealing times. The agglomeration rate increased as the crystallinity of the thin films increased [41].

3.3 Optical Properties

In order to examine the effects of time and temperature of post-deposition annealing on the properties of Cu_2ZnSnS_4 thin films, using Ultraviolet (UV) visible spectra in the 350–1000 nm wavelength range, absorption spectra were analyzed. The optical properties, such as absorbance and transmittance, were measured. These properties were studied on ITO substrates. One of the most important of these characteristics was the optical band gap, with values obtained for all CZTS annealed samples by the Tauc method. The direct band gap for the CZTS film was obtained by extrapolating the linear part of Tauc's curve to the intercept at the x = 0 axis after plotting the $(\alpha hv)^2$ evolution with (hv), as described in Eqn. 12 [43].

$$(\alpha hv)^2 = B\,(hv - E_g) \tag{12}$$

where B is constant. α represents the coefficient of absorption while h represents the Planck constant.

Fig. 5 displays the band gap of annealed samples at various temperatures. For CZTS deposited at T = 150, 200, 250, and 300 ºC, the corresponding band gap (Eg) values were 1.69, 1.66, 1.50, and 1.43 eV. The synthesized CZTS thin layer at T = 250 ºC had the band gap energy that was closer to the absorber theoretical value (1.5 eV).

Fig. 6 displays Tauc plot for CZTS samples annealed at 250 ºC for different annealing times. According to estimates, the band gap values for 60, 90, and 120 min were 1.80, 1.50, and 1.30 eV, respectively. As the annealing time increased, the optical band gap was narrower, indicating that extended annealing improves the optical properties of CZTS. Tables 3,4 summarize these results. Interestingly, the samples obtained at a high annealing temperature of 250 ºC for 90 min revealed the formation of CZTS with an energy band gap of 1.50 eV. A band gap of 1.3 eV was obtained when annealing another sample at 250 ºC for 120 min.

The outcomes of the absorption study revealed that all samples exhibited absorption in the visible area. Visual absorbance of CZTS specimens that were annealed at 250 ºC for 60, 90, and 120 min, respectively, confirmed the film's suitability for future solar cell applications.

The Moss relation [41], Eqn. 13, clearly identifies the refractive index n with the major vitality band gap (E_g).

$$E_g n^4 = k \tag{13}$$

k is a constant equal to 108 eV. A distinct relation between the band gap energy and the refractive index was provided by Herve and Vandamme [18], Eqn. 14:

$$n^2 = 1 + \left(\frac{A}{E_g + B}\right)^2 \tag{14}$$

where the numerical constants A and B have corresponding values of 13.6 and 3.4 eV, respectively.

Each film underwent an evaluation of its high-frequency and static dielectric constants. The ε_0 static dielectric constant was determined using the accompanying relationship condition in Eqn. 15.

$$\varepsilon_0 = n^2 \tag{15}$$

where the refractive index is denoted by n. The band gap depends on ε_∞ the high recurrence dielectric constants of the films that were evaluated using Eqn. 16.

$$\varepsilon_\infty = 18.52 - 3.08 E_g \tag{16}$$

4. Discussion

4.1 Structural and Morphological Analysis

Commonly used XRD peaks to identify the kesterite CZTS phase are the (112) signal at 2θ = 28.4°, (220)/(204) near 47°, and (312)/(116) near 56°. However, it can be challenging to distinguish these signals using XRD alone

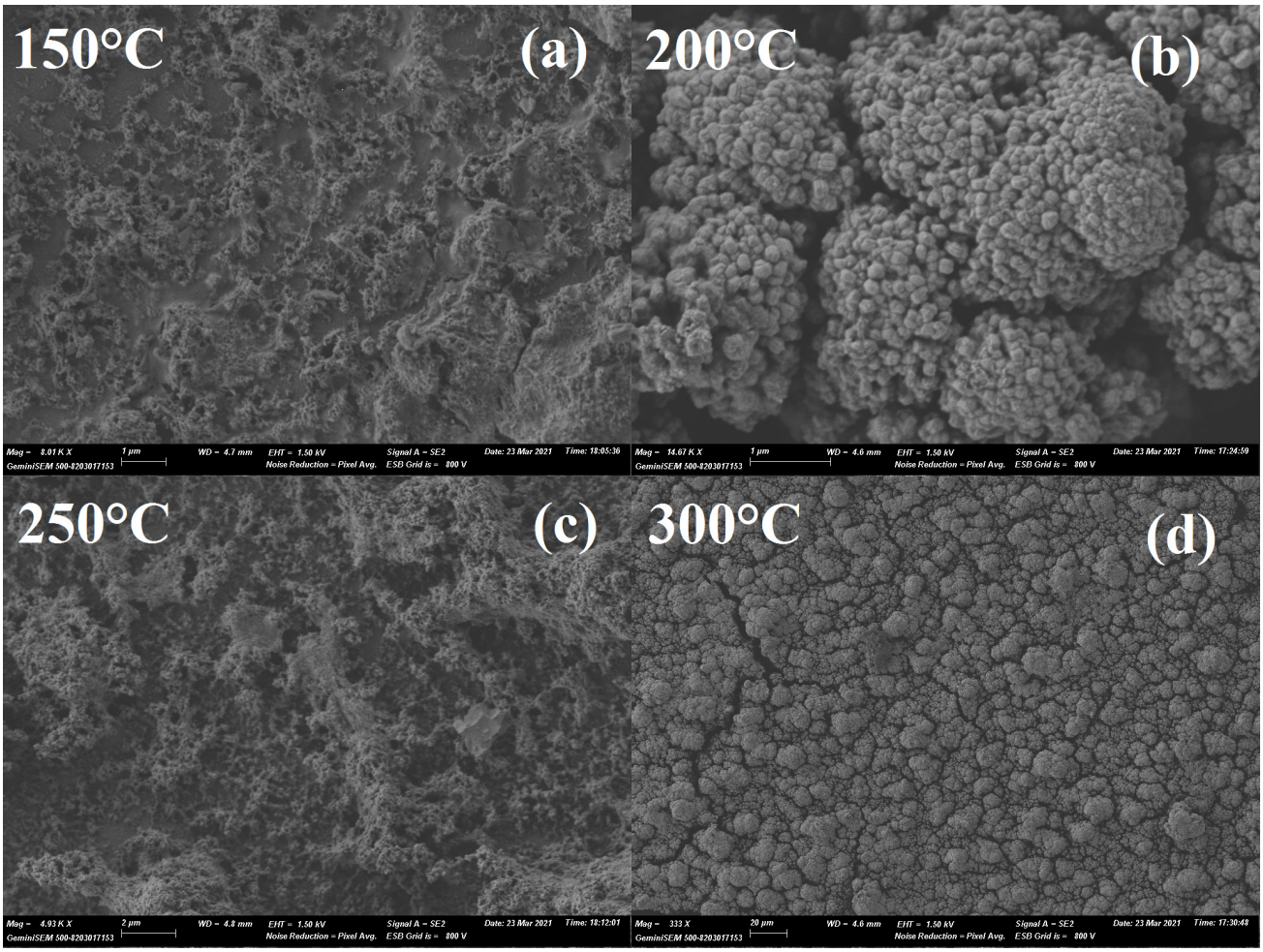

Fig. 4. The qualitative SEM analysis images of CZTS thin film annealed at different annealing temperatures, (a) in 150 ºC, (b) in 200 ºC, (c) in 250 ºC, and (d) in 300 ºC. SEM, scanning electron microscopy. Scale bar = 1 μm in (a,b); scale bar = 2 μm in (c); scale bar = 20 μm in (d).

Table 3. Impact of annealing temperature on the optical characteristics of thin-film CZTS annealed for 90 min.

Temperature annealing	Energy band (eV)	*n* Refractive index		ε_∞ High frequency dielectric constant	ε_0 Static dielectric
		Herve and Vandamme	Moss		
150 °C	1.69	2.852	2.827	7.994	13.314
200 °C	1.66	2.867	2.840	8.065	13.407
250 °C	1.50	2.950	2.912	8.485	13.900
300 °C	1.43	2.988	2.947	8.690	14.115

Table 4. Impact of annealing time on the optical characteristics of thin-film CZTS annealed at 250 ºC.

Time annealing	Energy band (eV)	*n* Refractive index		ε_∞ High frequency dielectric constant	ε_0 Static dielectric
		Herve and Vandamme	Moss		
60 min	1.80	2.8050	2.783	7.840	12.976
90 min	1.50	2.939	2.903	8.640	13.838
120 min	1.30	3.061	3.019	9.373	14.516

because they frequently overlap with those of secondary phases like Cu_2SnS_3 (CTS), ZnS, and SnS. Particularly at lower annealing temperatures or non-ideal stoichiometries [44], secondary phases such as Cu–S and Sn–S compounds can exhibit weak or broad signals that may be obscured by the dominant CZTS reflections. The main reflections of CZTS, (112), (220), and (312), overlap with those of ZnS (at 2θ 28.5, 47.5, and 56.3º), making it impossible to mea-

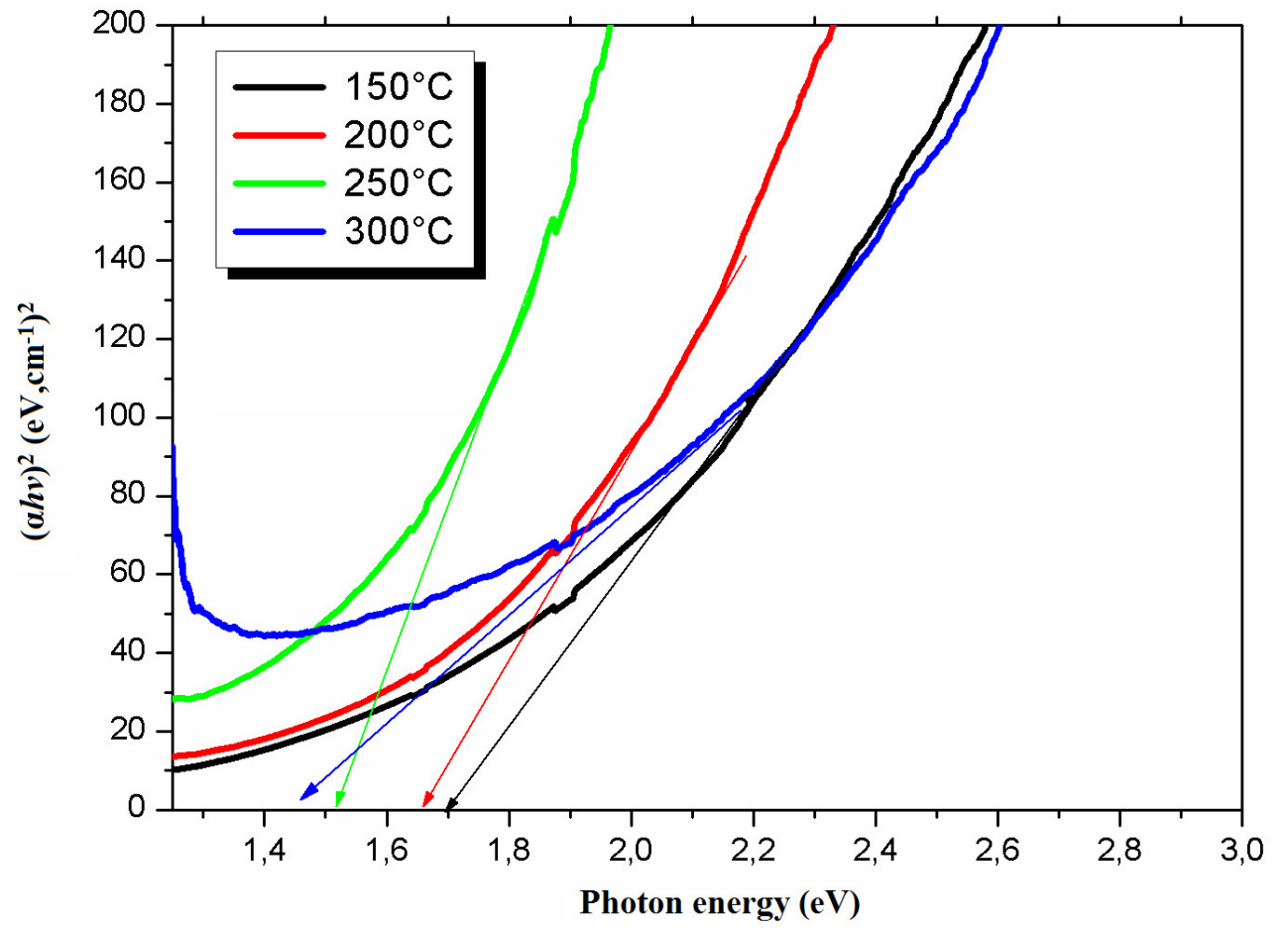

Fig. 5. Tauc plot of CZTS samples that were annealed at various temperatures.

sure without Rietveld refinement or high-resolution grazing incidence XRD. Cu_2S has a clear signal at about 2θ = 46.3°, which is different from that of CZTS at about 47.3°. The SnS/SnS_2 signals are broad and small [45]. When the annealing temperature goes up, the number of secondary phases tends to decrease. This sharpens the XRD reflections and makes the crystals purer, which means that CZTS is forming more clearly. Surface-sensitive methods show that secondary phases like CuS, ZnS, and SnS tend to build up close to the film surface in a thin layer. This may not have a big effect on bulk XRD signals [46]. Additionally, the technique resulted in a more homogeneous, compact, and smooth surface morphology with larger grains (see Fig. 4), which is advantageous for charge transmission [32].

4.2 Optical Properties and Band gap Tuning

In general, air annealing of CZTS thin films produced by the SILAR process improved crystallinity and grain growth, reduced secondary phases, and raised the purity of the CZTS phase. Annealing in air at moderate temperatures also reduced the band gap from 1.8 eV to 1.3 eV. This indicates changes in crystal structure and defect states that enhanced the quality of the film [32]. Improved crystal structure is confirmed by X-ray diffraction experiments following air annealing. Moreover, higher temperature annealing under sulfur atmospheres (400–450 ºC) significantly enhanced crystallinity and band gap [31,47]. On the flip side, air annealing can enhance Cu–Zn ordering, raise absorber band gap energy, and encourage elemental intermixing at interfaces (such as CZTS/CdS). These actions may increase the open-circuit voltage of the device, but they may also produce Cu-rich surface layers that, if unchecked, may reduce the performance of the solar cell [48].

The modified SILAR approach was used in this study to create CZTS nanoparticles. A band gap of 1.3 eV was obtained when annealing another sample at 250 ºC for 120 min. Whereas Shinde et al. [32] get a ban dgap of 1.5–1.8 eV 4 h at high temperatures, this is a remarkable progress in lowering time and temperature annealing, and thus reducing the cost in this work. This confirms the effectiveness of the added phase in the present work.

The synthesized CZTS thin layer at T = 250 ºC had the band gap energy that was closer to the absorber theoretical value (1.5 eV). The same change in the band gap energy trend was noted by Kahraman et al. [49] for CZTS deposited at high sulfurized temperatures.

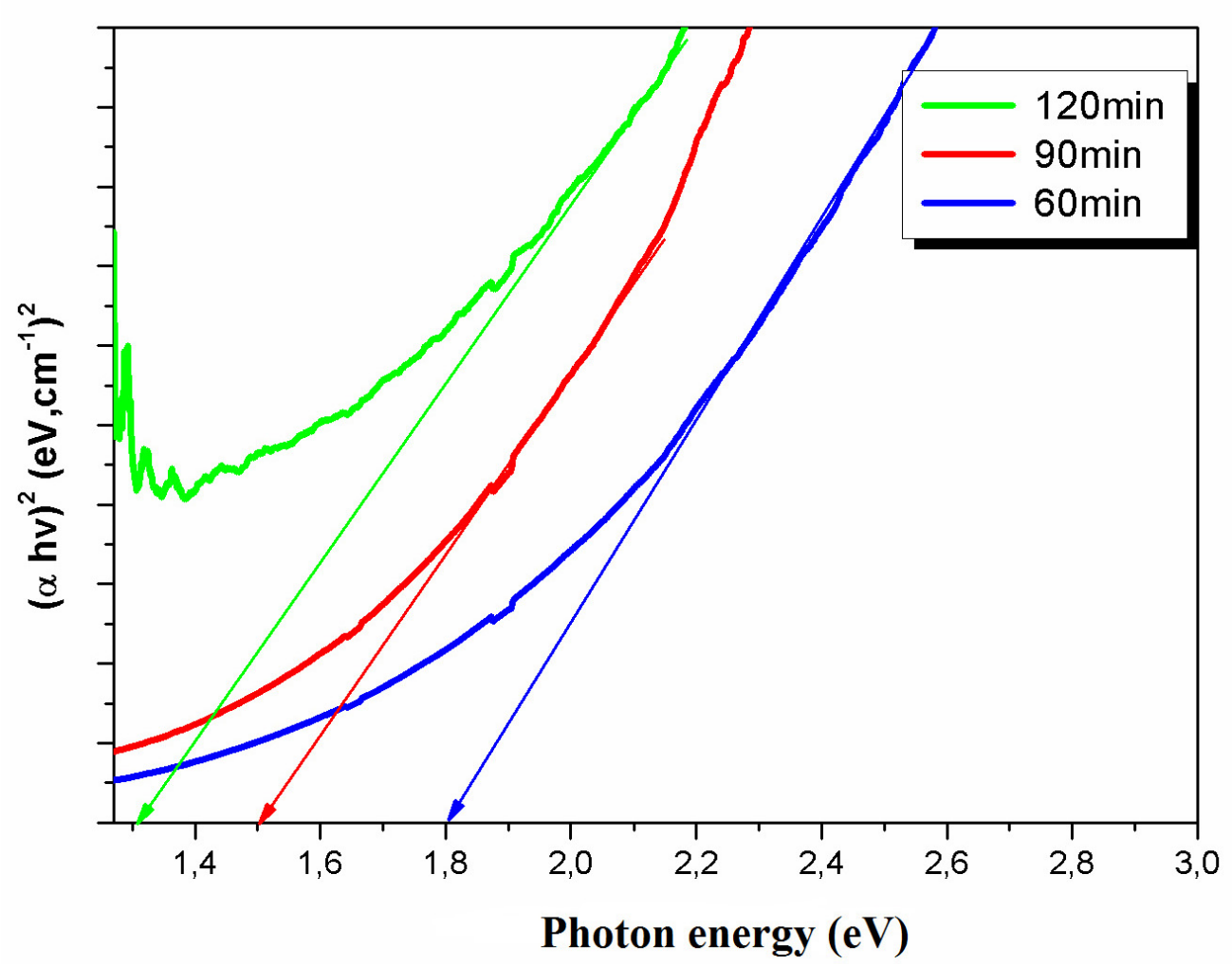

Fig. 6. Tauc plot of CZTS samples, annealed at 250 ºC for varied annealing durations.

As in most experimental papers, the present study indicates that increasing annealing time and temperature decreases the band gap. This is primarily due to sulfur loss, Cu–Zn disorder, and stoichiometric changes that collectively enhance band tailing and introduce sub-gap states, thereby reducing the effective band gap. Similar to this, Henry et al. [18] used SILAR to create CZTS nanoparticles that had a large peak located along (2 2 0) and (1 1 2).

In the study of CZTS, observing a reduction in the optical band gap with increased temperature and time is a very common and well-documented trend. This "narrowing" of the band gap is usually interpreted through primary physical mechanisms, where sulfur loss, defect reduction, and Cu–Zn disorder are all impacted by increasing the annealing temperature and duration. These factors ultimately affect the band gap. Higher annealing temperatures (about 550–580 ºC) enhance crystallinity and increase Cu–Zn disorder, resulting in a more disordered kesterite structure and a narrow band gap, which normally decreases with rising temperature and longer annealing time under a sulfur atmosphere [9]. Sulfur loss occurs at high annealing durations or temperatures, resulting in secondary phases and compositional deviations such as Sn or Zn loss, which can narrow the band gap due to defect states or impurity phases like Cu_2SnS_3 or Cu_2-xS [50,51].

Optimal annealing reduces defects and non-radiative recombination centers, which leads to a cleaner band gap closer to the ideal kesterite value (~1.5 eV) [52]. As the annealing temperature rises, Cu–Zn disorder increases, which broadens the optical absorption edge and decreases the effective band gap [9] by disorder-induced band tailing and defect-related states near the band edges. However, too long sulfurization durations might result in the development of secondary phases, such as SnS_2, which can have a detrimental effect on band gap uniformity [53] and film quality. Overall, to optimize the CZTS band gap for solar performance, controlled annealing strikes a compromise between cation ordering, sulfur retention, and defect passivation [51,54].

Table 5 (Ref. [18,41,47]) compares the empirically acquired values in the model (modified SILAR) with those reported using standard SILAR. We employed much fewer

Table 5. Comparison between the modified SILAR model and the experimentally reported values from conventional SILAR.

	Conventional SILAR method			Modified SILAR method	
References	[47]	[18]	[41]	Best results in this work	
Band gap Eg (eV)	1.50	1.54	1.51	1.5	1.3
Cycles number	100	70	100	50	50
Annealing time (min)	10	120	60	90	120
Annealing conditions	in air	under sulphur	in air	in air	in air
Temperature (ºC)	250	500	400	250	250

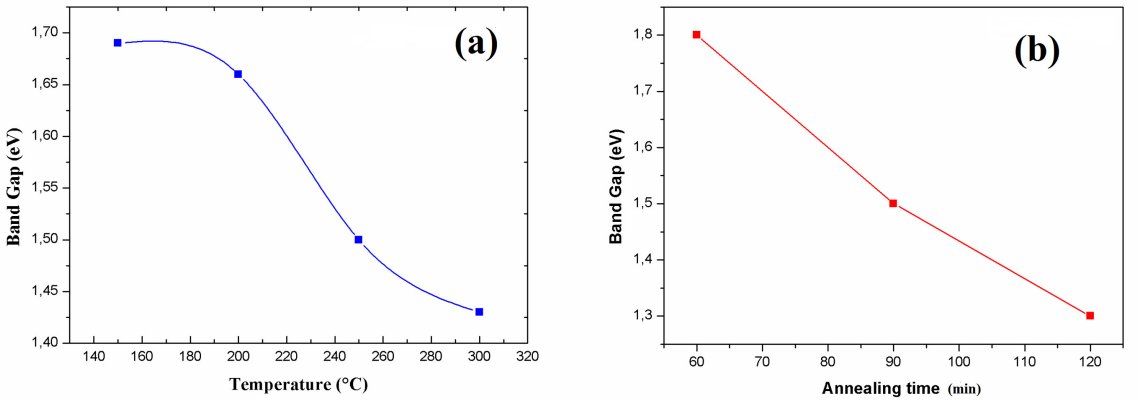

Fig. 7. Band gap of CZTS thin films variation with (a) annealing temperature, (b) time of annealing.

cycles and shorter annealing times to attain the optimal performance of the proposed optical property compared to the values reported in the literature [30,41,47,55]. This improvement was actually caused by the extra heating step. According to these results, the proposed method provided a low-cost, non-toxic means of creating optimized CZTS absorbers that may be used at low temperatures.

Fig. 7 demonstrates that extending the annealing time from 60 to 120 minutes resulted in a band gap decrease. This narrowing is primarily attributed to enhanced Cu–Zn cationic disorder and stoichiometric deviations. Additionally, the CZTS film Tauc plot annealed for 90 min at various annealing temperatures is shown in Fig. 7a. Thus, the band gaps (*Eg*) were 1.69, 1.66, 1.50 and 1.43 eV for 150, 200, 250, and 300 ºC, respectively. Notably, similar results were obtained in the literature, but at higher temperatures and for an extended length of time, indicating the effectiveness of the additive phase (the new step) here. The study by El Mahboub et al. [56] found that increasing the annealing temperature for spin-coated CZTS thin films reduced the optical band gap. In particular, their research on sol-gel spin-coated and electrodeposited films showed that the band gap energy narrowed from values about 1.65–1.72 eV to roughly 1.50–1.56 eV as the annealing temperature rose from lower ranges (e.g., 350 ºC) toward ideal levels (400–500 ºC). In other experiments [57], recent characterizations of sputtered copper zinc tin sulfide (CZTS) thin films have confirmed that the annealing temperature is the key lever for adapting the optical band gap. The band gap for these sputtered absorbers usually narrows from as high as 1.7–1.8 eV to the optimal bulk value of ~1.45–1.50 eV when the annealing temperature is raised from 300 to 550 ºC. Obviously, the band gap decreases as the annealing temperature increases (Fig. 7a). This is due to enhanced Cu–Zn cationic disorder and stoichiometric deviations (including sulfur loss) at elevated temperatures, which reduce the effective band gap, according to previously reported findings [25,31,55,58]. Furthermore, the CZTS samples showed the best results when they were annealed at 250 and 200 ºC for 90 minutes and 120 minutes, respectively. This resulted in a band gap of 1.5 eV, which is in good congruence with literature [59,60]. This direct material band gap value is perfect for usage in solar energy systems as the absorber layer.

4.3 Limitations

Based on the results obtained in this study, several limitations and challenges are expected when using CZTS composite thin films in solar cells, despite the efficiency of the new SILAR modification in reducing heat and annealing time. However, some limitations remain, the most significant being sulfur loss.

The findings showed variations in the material chemical ratios and sulfur loss when samples were annealed in air at high temperatures and for long periods of time. When this sulfur evaporates, sulfur voids or unwanted secondary phases like ZnS or Cu_2S occur, which impairs the light-absorbing layer's function.

Additionally, the results demonstrated that the band gap is highly sensitive to any change in time (from 60 to 120 minutes) or temperature (from 150 to 300 °C), decreasing

from 1.69 to 1.43 eV; this is due to the difficulty of precisely controlling these parameters (reproducibility) during large-scale commercial manufacturing. Even slight fluctuations in annealing temperature or curing time will result in films with varying energy gaps, impacting production reliability. A new challenge has emerged: finding the optimal balance between temperature and time. We achieved the best results (an optimal energy gap of 1.5 eV) at a specific combination (250 °C for 90 minutes). Therefore, reducing the temperature would require extending the curing time to more than two hours, which may not be economically viable for fast factory production lines.

Finally, although the described method has successfully reduced the temperature required for annealing compared to previous studies (which reached 550 °C), controlling crystal defects remains the greatest obstacle to increasing the efficiency of these cells.

5. Conclusions

In this work, using a modified SILAR technique at low temperatures, CZTS films were deposited on ITO substrates. The temperature for annealing was adjusted from 150 to 300 ºC, and the annealing duration was extended from 60 to 120 min to investigate the effects of annealing parameters on the optical characteristics of CZTS films. The XRD signals for (112), (220), and (312) were present in all of the as-deposited CZTS films, suggesting that they all contain a kesterite structure. Additionally, the absorbance of the CZTS films significantly increased with the annealing temperature from 150 to 300 ºC and the annealing period from 60 to 120 min. The CZTS film optical band gap shrank from 1.69 to 1.43 eV and approached the ideal value needed for a substance that absorbs in solar cells at various periods and from 1.80 to 1.30 eV at various annealing temperatures. The CZTS films produced after annealing at 250 ºC for 90 min or 250 ºC for 120 min showed remarkable potential for the creation of high-quality CZTS thin films in thin-film solar cells with an optimal band gap of 1.5 and 1.3 eV, respectively. The CZTS films formed using the modified SILAR approach are appropriate for photovoltaic devices. By incorporating this change into the traditional SILAR methods, a low annealing temperature, a basic medium, and a restricted number of cycles can all yield acceptable outcomes. As a result, there is reduced cost and complexity. However, the method still has drawbacks, such as potential issues with phase purity and crystal quality degradation. Since the initial results are so encouraging, we are keen to conduct additional research and development to improve the process and deliver the optimized results.

Availability of Data and Materials

Data will be available from the corresponding author on reasonable request.

Author Contributions

TT: Writing–original draft, Methodology, Investigation. HK: review & editing, Supervision, Project administration, analysis, and interpretation of data. FS: interpretation of results, Investigation, Formal analysis. NS: Writing, drafted the manuscript and critically reviewed it for substantial intellectual content & editing, validation. BMS: Direction of the experimental part, review & editing. AL: Methodology. MT: Review, investigation and interpretation of data for the work & editing. All authors contributed to editorial changes in the manuscript. All authors read and approved the final manuscript. All authors have participated sufficiently in the work and agreed to be accountable for all aspects of the work.

Ethics Approval and Consent to Participate

Not applicable.

Acknowledgment

Special thanks to Professor Hikmat S. Hilal, SSERL, Department of Chemistry, An-Najah National University, Nablus, Palestine, for his great assistance in improving the language of the manuscript. T. Tahouri thanks Amar Telidji University-Laghouat, and Tahri Mohammed University - Béchar for support. Authors also thank the General Directorate of Scientific Research & Technological Development (DGRSDT), Algeria.

Funding

This research received no external funding.

Conflicts of Interest

The authors declare no conflicts of interest.

References

[1] Green M, Dunlop E, Yoshita M, Kopidakis N, Bothe K, Siefer G, et al. Solar Cell Efficiency Tables (Version 66). Progress in Photovoltaics: Research and Applications. 2025; 33: 795–810. https://doi.org/10.1002/pip.3919

[2] Selmane N, Cheknane A, Hilal HS. A new CsPbI2Br/CuZnSnSSe/Si tandem solar cell with higher than 32 % efficiency. Micro and Nanostructures. 2024; 194: 207940. https://doi.org/10.1016/j.micrna.2024.207940

[3] Afrah BF, Naceur S, Ali C, Fakhereddine K, Bsharat H, Hilal HS. Cost-lowering and performance-improvement of B-γ-CsSnI3 solar cells by adding CZTSSe absorber. Journal of Electroanalytical Chemistry. 2025; 996: 119369. https://doi.org/10.1016/j.jelechem.2025.119369

[4] Boukhelkhal FA, Selmane N, Cheknane A, Noureddine M, Zoukel A, Baydogan N, et al. Ecofriendly high-performance low-cost Cu2ZnSnSe4 solar cells: Experimental characterization and SCAPS-1D simulation. Chemical Physics. 2026; 601: 112952. https://doi.org/10.1016/j.chemphys.2025.112952

[5] Nakamura M, Yamaguchi K, Kimoto Y, Yasaki Y, Kato T, Sugimoto H. Cd-Free Cu(In,Ga)(Se,S) 2 Thin-Film Solar Cell With Record Efficiency of 23.35%. The IEEE Journal of Photovoltaics. 2019; 9: 1863–1867. https://doi.org/10.1109/JPHOTOV.2019.2937218

[6] Shockley W, Queisser HJ. Detailed Balance Limit of Efficiency of p-n Junction Solar Cells. Journal of Applied Physics. 1961; 32: 510–519. https://doi.org/10.1063/1.1736034
[7] Ocak YS, Bayansal F. Advancing Earth-Abundant CZTSSe Solar Cells: Recent Progress in Efficiency and Defect Engineering. Nanomaterials (Basel, Switzerland). 2025; 15: 1617. https://doi.org/10.3390/nano15211617
[8] Babichuk IS, Semenenko MO, Golovynskyi S, Caballero R, Datsenko OI, Babichuk IV, et al. Control of secondary phases and disorder degree in Cu2ZnSnS4 films by sulfurization at varied subatmospheric pressures. Solar Energy Materials and Solar Cells. 2019; 200: 109915. https://doi.org/10.1016/j.solmat.2019.109915
[9] Choudhari NJ, Raviprakash Y, Bellarmine F, Ramachandra Rao MS, Pinto R. Investigation on the sulfurization temperature dependent phase and defect formation of sequentially evaporated Cu-rich CZTS thin films. Solar Energy. 2020; 201: 348–361. https://doi.org/10.1016/j.solener.2020.03.007
[10] Fontané X, Calvo-Barrio L, Izquierdo-Roca V, Saucedo E, Pérez-Rodriguez A, Morante JR, et al. In-depth resolved Raman scattering analysis for the identification of secondary phases: Characterization of Cu2ZnSnS4 layers for solar cell applications. Applied Physics Letters. 2011; 98: 181905. https://doi.org/10.1063/1.3587614
[11] Ren G, Zhuang D, Zhao M, Wei Y, Wu Y, Li X, et al. Influences of Cu concentration on electrical properties of CZTSSe absorbers and their device performances. Vacuum. 2020; 173: 109121. https://doi.org/10.1016/j.vacuum.2019.109121
[12] Olgar MA, Atasoy Y, Başol BM, Tomakin M, Aygun G, Ozyuzer L, et al. Influence of copper composition and reaction temperature on the properties of CZTSe thin films. Journal of Alloys and Compounds. 2016; 682: 610–617. https://doi.org/10.1016/j.jallcom.2016.04.309
[13] Olgar MA, Klaer J, Mainz R, Levcenco S, Just J, Bacaksiz E, et al. Effect of precursor stacking order and sulfurization temperature on compositional homogeneity of CZTS thin films. Thin Solid Films. 2016; 615: 402–408. https://doi.org/10.1016/j.tsf.2016.07.058
[14] Dimitrievska M, Fairbrother A, Izquierdo-Roca V, Perez-Rodriguez A, Saucedo E. Two ideal compositions for kesterite-based solar cell devices. In 2014 IEEE 40th Photovoltaic Specialist Conference (PVSC) (pp. 2307–2309). IEEE: Denver, CO, USA. 2014. https://doi.org/10.1109/PVSC.2014.6925387
[15] Vermang B, Wätjen JT, Fjällström V, Rostvall F, Edoff M, Kotipalli R, et al. Employing Si solar cell technology to increase efficiency of ultra-thin Cu(In,Ga)Se_2 solar cells. Progress in Photovoltaics: Research and Applications. 2014; 22: 1023–1029. https://doi.org/10.1002/pip.2527
[16] Liu F, Huang J, Sun K, Yan C, Shen Y, Park J, et al. Beyond 8% ultrathin kesterite Cu2ZnSnS4 solar cells by interface reaction route controlling and self-organized nanopattern at the back contact. NPG Asia Materials. 2017; 9: e401–e401. https://doi.org/10.1038/am.2017.103
[17] Mahajan S, Stathatos E, Huse N, Birajdar R, Kalarakis A, Sharma R. Low cost nanostructure kesterite CZTS thin films for solar cells application. Materials Letters. 2018; 210: 92–96. https://doi.org/10.1016/j.matlet.2017.09.001
[18] Henry J, Mohanraj K, Sivakumar G. Electrical and Optical Properties of CZTS Thin Films Prepared by SILAR Method. Journal of Asian Ceramic Societies. 2016; 4: 81–84. https://doi.org/10.1016/j.jascer.2015.12.003
[19] Sankapal BR, Mane RS, Lokhande CD. Deposition of CdS thin films by the successive ionic layer adsorption and reaction (SILAR) method. Materials Research Bulletin. 2000; 35: 177–184. https://doi.org/10.1016/S0025-5408(00)00210-5
[20] Chandra PP, Mukherjee A, Mitra P. Synthesis of Nanocrystalline CdS by SILAR and their Characterization. Journal of Materials. 2014; 2014: 1–6. https://doi.org/10.1155/2014/138163
[21] Jose E, Santhosh Kumar MC. Room Temperature Deposition of Highly Crystalline Cu-Zn-S Thin Films for Solar Cell Applications Using SILAR Method. Journal of Alloys and Compounds 2017; 712: 649–656. https://doi.org/10.1016/j.jallcom.2017.04.097
[22] Su Z, Sun K, Han Z, Liu F, Lai Y, Li J, et al. Fabrication of Ternary Cu–Sn–S Sulfides by a Modified Successive Ionic Layer Adsorption and Reaction (SILAR) Method. Journal of Materials Chemistry. 2012; 22: 16346. https://doi.org/10.1039/c2jm31669b
[23] Nicolau YF. Solution deposition of thin solid compound films by a successive ionic-layer adsorption and reaction process. Applications of Surface Science. 1985; 22-23: 1061–1074. https://doi.org/10.1016/0378-5963(85)90241-7
[24] Suryawanshi MP, Shin SW, Ghorpade UV, Gurav KV, Agawane GL, Hong CW, et al. A chemical approach for synthesis of photoelectrochemically active Cu 2 ZnSnS 4 (CZTS) thin films. Solar Energy. 2014; 110: 221–230. https://doi.org/10.1016/j.solener.2014.09.008
[25] Maheswari B, Dhanam M. Optimization of Deposition Temperature of SILAR Cu-Rich CuInS2 Thin Films. Materials Science-Poland. 2013; 31: 193–200. https://doi.org/10.2478/s13536-012-0094-0
[26] Pathan HM, Lokhande CD. Deposition of metal chalcogenide thin films by successive ionic layer adsorption and reaction (SILAR) method. Bulletin of Materials Science. 2004; 27: 85–111. https://doi.org/10.1007/BF02708491
[27] Shinde NM, Dubal DP, Dhawale DS, Lokhande CD, Kim JH, Moon JH. Room temperature novel chemical synthesis of Cu2ZnSnS4 (CZTS) absorbing layer for photovoltaic application. Materials Research Bulletin. 2012; 47: 302–307. https://doi.org/10.1016/j.materresbull.2011.11.020
[28] Mali SS, Patil BM, Betty CA, Bhosale PN, Oh YW, Jadkar SR, et al. Novel synthesis of kesterite Cu2ZnSnS4 nanoflakes by successive ionic layer adsorption and reaction technique: Characterization and application. Electrochimica Acta. 2012; 66: 216–221. https://doi.org/10.1016/j.electacta.2012.01.079
[29] Znaidi L, Diyagh H, Benaicha I, Bouri N, Gana LE, Farri HE, et al. Effect of Bath Temperature on Physical Properties of Thin Films CuO Using the SILAR Method: Photocatalytic Properties and Numerical Investigation. Chemical Physics Impact. 2025; 11: 100901. https://doi.org/10.1016/j.chphi.2025.100901
[30] Patwary MAM, Hossain MA, Ghos BC, Chakrabarty J, Haque SR, Rupa SA, et al. Copper oxide nanostructured thin films processed by SILAR for optoelectronic applications. RSC Advances. 2022; 12: 32853–32884. https://doi.org/10.1039/d2ra06303d
[31] Chen L, Park C. Effects of annealing temperature on Cu2ZnSnS4 (CZTS) films formed by electrospray technique. Korean Journal of Chemical Engineering. 2017; 34: 1187–1191. https://doi.org/10.1007/s11814-017-0011-7
[32] Shinde NM, Deshmukh PR, Patil SV, Lokhande CD. Aqueous chemical growth of Cu2ZnSnS4 (CZTS) thin films: Air annealing and photoelectrochemical properties. Materials Research Bulletin. 2013; 48: 1760–1766. https://doi.org/10.1016/j.materresbull.2012.12.053
[33] Han C, Han S, Gwak J, Khatkar SP. Synthesis of indium tin oxide (ITO) and fluorine-doped tin oxide (FTO) nano-powder by sol–gel combustion hybrid method. Materials Letters. 2007; 61: 1701–1703. https://doi.org/10.1016/j.matlet.2006.07.114
[34] Manafi S, Tazikeh S, Joughehdoust S. Synthesis and characterization of indium tin oxide nanoparticles via reflux method. Materials Science-Poland. 2017; 35: 799–805. https://doi.org/10.1515/msp-2018-0008

[35] Zaki MY, Velea A. Recent progress and challenges in controlling secondary phases in kesterite CZT (S/Se) thin films: A critical review. Energies. 2024; 17: 1600. https://doi.org/10.3390/en17071600
[36] Jay Chithra M, Sathya M, Pushpanathan K. Effect of pH on Crystal Size and Photoluminescence Property of ZnO Nanoparticles Prepared by Chemical Precipitation Method. Acta Metallurgica Sinica (English Letters). 2015; 28: 394–404. https://doi.org/10.1007/s40195-015-0218-8
[37] Al-Bataineh QM, Telfah M, Ahmad AA, Alsaad AM, Qattan IA, Baaziz H, et al. Synthesis, crystallography, microstructure, crystal defects, optical and optoelectronic properties of ZnO: CeO2 mixed oxide thin films. Photonics. 2020; 7: 112. https://doi.org/10.3390/photonics7040112
[38] Yeh MY, Lei PH, Lin SH, Yang CD. Copper-Zinc-Tin-Sulfur Thin Film Using Spin-Coating Technology. Materials (Basel, Switzerland). 2016; 9: 526. https://doi.org/10.3390/ma9070526
[39] Mrabet C, Boukhachem A, Amlouk M, Manoubi T. Improvement of the optoelectronic properties of tin oxide transparent conductive thin films through lanthanum doping. Journal of Alloys and Compounds. 2016; 666: 392–405. https://doi.org/10.1016/j.jallcom.2016.01.104
[40] Williamson GK, Smallman RE. III Dislocation densities in some annealed and cold-worked metals from measurements on the X-ray debye-scherrer spectrum. Philosophical Magazine. 1956; 1: 34–46. https://doi.org/10.1080/14786435608238074
[41] Murugan A, Siva V, Shameem A, Asath Bahadur S. Preparation of Cu2ZnSnS4 Thin Films by Successive Ionic Layer Adsorption and Reaction (SILAR) Method for Supercapacitor Applications. Journal of Nanoscience and Nanotechnology. 2020; 20: 6235–6244. https://doi.org/10.1166/jnn.2020.17888
[42] Islam MA, Hossain MS, Aliyu MM, Karim MR, Razykov T, Sopian K, et al. Effect of CdCl2 treatment on structural and electronic property of CdTe thin films deposited by magnetron sputtering. Thin Solid Films. 2013; 546: 367–374. https://doi.org/10.1016/j.tsf.2013.04.067
[43] Cao M, Li L, Zhang BL, Huang J, Wang LJ, Shen Y, et al. One-step deposition of Cu2ZnSnS4 thin films for solar cells. Solar Energy Materials and Solar Cells. 2013; 117: 81–86. https://doi.org/10.1016/j.solmat.2013.05.039
[44] Olgar MA. Enhancement in photovoltaic performance of CZTS Thin-film solar cells through varying stacking order and sulfurization time. Journal of Materials Science: Materials in Electronics. 2022; 33: 20121–20133. https://doi.org/10.1007/s10854-022-08829-y
[45] Boerasu I, Vasile BS. Current Status of the Open-Circuit Voltage of Kesterite CZTS Absorber Layers for Photovoltaic Applications-Part I, a Review. Materials (Basel, Switzerland). 2022; 15: 8427. https://doi.org/10.3390/ma15238427
[46] Zhang X, Wu H, Fu E, Wang Y. In-Depth Characterization of Secondary Phases in Cu_2ZnSnS_4 Film and Its Application to Solar Cells. Nanomaterials (Basel, Switzerland). 2019; 9: 855. https://doi.org/10.3390/nano9060855
[47] Patel K, Shah DV, Kheraj V. Influence of deposition parameters and annealing on Cu2ZnSnS4 thin films grown by SILAR. Journal of Alloys and Compounds. 2015; 622: 942–947. https://doi.org/10.1016/j.jallcom.2014.11.019
[48] Gansukh M, Martinho F, Espindola M, Engberg S, Schou J, Canulescu S. The effect of post-annealing on the performance of the Cu_2ZnSnS_4 solar cells. Scientific Reports. 2024; 14: 19898. https://doi.org/10.1038/s41598-024-70865-x
[49] Kahraman S, Çetinkaya S, Podlogar M, Bernik S, Çetinkara HA, Güder HS. Effects of the sulfurization temperature on sol gel-processed Cu2ZnSnS4 thin films. Ceramics International. 2013; 39: 9285–9292. https://doi.org/10.1016/j.ceramint.2013.05.039
[50] Wu X, Yuan Y, Duan Y, Chen Y, Liu X. Improvement of Cu2ZnSnS4 films properties using sulfurized precursor films with Cu-poor/Zn-rich ratio. Journal of Solid State Chemistry. 2024; 333: 124641. https://doi.org/10.1016/j.jssc.2024.124641
[51] Olgar MA. Optimization of sulfurization time and temperature for fabrication of Cu2ZnSnS4 (CZTS) thin films. Superlattices and Microstructures. 2019; 126: 32–41. https://doi.org/10.1016/j.spmi.2018.12.012
[52] Olgar MA, Erkan S, Zan R. Dependence of CZTS thin film properties and photovoltaic performance on heating rate and sulfurization time. Journal of Alloys and Compounds. 2023; 963: 171283. https://doi.org/10.1016/j.jallcom.2023.171283
[53] Olgar MA, Seyhan A, Sarp AO, Zan R. Impact of sulfurization parameters on properties of CZTS thin films grown using quaternary target. Journal of Materials Science: Materials in Electronics. 2020; 31: 20620–20631. https://doi.org/10.1007/s10854-020-04582-2
[54] Vázquez-González PJ, Paniagua-Chávez ML, Zebadua-Chavarria LA, Mota-Grajales R, Meza-Avendaño CA, Campos-González E, et al. Comprehensive Structural, Chemical, and Optical Characterization of Cu_2ZnSnS_4 Films on Kapton Using the Automated Successive Ionic Layer Adsorption and Reaction Method. Nanomaterials (Basel, Switzerland). 2025; 15: 85. https://doi.org/10.3390/nano15020085
[55] Suryawanshi MP, Shin SW, Ghorpade UV, Gurav KV, Hong CW, Patil PS, et al. Improved solar cell performance of Cu2ZnSnS4 (CZTS) thin films prepared by sulfurizing stacked precursor thin films via SILAR method. Journal of Alloys and Compounds. 2016; 671: 509–516. https://doi.org/10.1016/j.jallcom.2016.02.015
[56] El Mahboub E, Zakaria S, El Hichou A, Mansori M. Impact of heating on the properties of CZTS thin film solar cells produced through sol-gel spin-coated. Nanomaterials and Energy. 2025; 14: 170–182. https://doi.org/10.1680/jnaen.24.00066
[57] Pandharkar S, Punde A, Nasane M, Doiphode V, Shinde P, Vairale P, et al. Soft Annealing Effect on the Properties of Sputter Grown Cu2ZnSnS4 (CZTS) Thin Films for Solar Cell Applications. Materials Today: Proceedings. 2021; 34: 690–696. https://doi.org/10.1016/j.matpr.2020.03.652
[58] Mahalakshmi V, Venugopal D, Ramachandran K, Ramesh R. Synthesis of 2D-CZTS nanoplate as photocathode material for efficient PEC water splitting. Journal of Materials Science: Materials in Electronics. 2022; 33: 8493–8503. https://doi.org/10.1007/s10854-021-06400-9
[59] Khalate SA, Kate RS, Deokate RJ. A review on energy economics and the recent research and development in energy and the Cu2ZnSnS4 (CZTS) solar cells: A focus towards efficiency. Solar Energy. 2018; 169: 616–633. https://doi.org/10.1016/j.solener.2018.05.036
[60] Ito K. Copper Zinc Tin Sulfide-Based Thin Film Solar Cells. 1st edn. Wiley: United Kingdom. 2015.